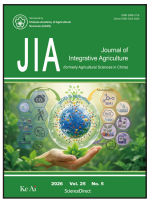
Journal of Integrative Agriculture 2026, 25(5): 2051–2062

Available online at ScienceDirect

Journal of Integrative Agriculture



RESEARCH ARTICLE

A candidate tick-borne encephalitis virus vaccine based on virus-like particles induces specific cellular and humoral immunity in mice

Mengyao Zhang, Hongli Jin, Cuicui Jiao, Yuanyuan Zhang, Yujie Bai, Zhiyuan Gong, Pei Huang, Haili Zhang, Yuanyuan Li#, Hualei Wang#

State Key Laboratory for Diagnosis and Treatment of Severe Zoonotic Infectious Diseases/Key Laboratory for Zoonosis Research of Ministry of Education, Institute of Zoonosis, College of Veterinary Medicine, Jilin University, Changchun 130062, China

Highlights

- Tick-borne encephalitis virus VLPs were prepared by expression of TBEV-prM-E protein using a baculovirus expression system.
- TBEV VLPs induced specific cellular and humoral immunity in mice.
- The TBEV VLPs vaccine was enabled as a TBEV vaccine candidate.

Abstract

Tick-borne encephalitis (TBE) is an important zoonotic viral disease transmitted by ticks. In recent decades, global climate change has increased human exposure to ticks, and mortality rate have gradually risen. Effective vaccines are essential for controlling TBE as specific antiviral treatment is unavailable. Vaccine candidates based on virus-like particles (VLPs) have previously been demonstrated to be effective in eliciting excellent immune responses against influenza virus and SARS-CoV-2. Here, we constructed TBE virus (TBEV) VLPs containing the envelope and membrane proteins derived from the Far Eastern TBEV strain (WH2012) using an insect cell-baculovirus expression system. Induction of immune responses was investigated in mice following intramuscular injection with the TBEV VLPs vaccine candidates formulated with a combination of poly(I:C) and Montanide ISA201VG adjuvants. Mice produced memory T-cells and serum-specific IgG antibodies that averaged up to $1:10^{4.6}$ and remained at $1:10^{4}$ (mean) at 24 wk after three immunizations. TBEV VLPs vaccine was able to provide long-term antibody protection against TBEV, making it a promising subunit vaccine candidate for this disease.

Keywords: tick-borne encephalitis virus, virus-like particles, envelope protein, subunit vaccine

1. Introduction

Tick-borne encephalitis (TBE) is a disease of the nervous system of humans and other animals infected by a tick-borne encephalitis virus (TBEV) (Slunge *et al.* 2022). Symptoms are usually confined to a febrile illness, but infection may lead to severe neurological sequelae (Taba *et al.* 2017). TBE seriously threatens human and public health security, which is the most prevalent arboviral disease affecting the human central nervous system in Europe and Northeast Asia (Ruzek *et al.* 2019). In recent years, TBE has taken on new epidemiological characteristics. For example, new areas of epidemic focus continue to emerge, as the ranges of the virus-transmitting vectors, ticks, expand under the influence of global climate change (Süss 2011; Fares *et al.* 2021; Esser *et al.* 2022). Moreover, new subtypes of TBEV have emerged (Demina *et al.* 2010; Dai *et al.* 2018), and the incidence of the disease has been increasing in established areas of epidemic focus (Donoso Mantke *et al.* 2011; Slunge *et al.* 2022). Vaccine immunization is essential for the preventive control of TBE since no specific antiviral treatment is available.

All five commercially available vaccines against TBEV are inactivated vaccines (Loew-Baselli *et al.* 2006; Xing *et al.* 2017). Due to the inability to infect cells, inactivated vaccines are more likely to activate $CD4^+$ T cells compared to $CD8^+$ T cells. Consequently, it is difficult to generate a $CD8^+$ T cell response without the aid of adjuvants (Bungener *et al.* 2008;

Received 2 March 2024; Received in revised form 28 June 2024; Accepted 21 July 2024; Available online 26 September 2024
#Correspondence Hualei Wang, E-mail: wanghualei@jlu.edu.cn; Yuanyuan Li, E-mail: li_yuanyuan@jlu.edu.cn

© 2026 CAAS. Publishing services by Elsevier B.V. on behalf of KeAi Communications Co. Ltd. This is an open access article under the CC BY-NC-ND license (http://creativecommons.org/licenses/by-nc-nd/4.0/). Peer review under responsibility of Editorial Board of *Journal of Integrative Agriculture*.
doi: 10.1016/j.jia.2024.09.024

Palomino-Tapia *et al.* 2019; Li *et al.* 2022; Lim *et al.* 2022; Liu *et al.* 2022; Zhang and Cui 2023). As a zoonotic pathogen, TBEV imposes stringent environmental requirements for the production of inactivated vaccines (Kunz *et al.* 1976; Kubinski *et al.* 2020), which can increase production costs and pose a health risk to operators (Zimna *et al.* 2023). In addition, there are the disadvantages of multiple immunizations and the limited duration of effective protection.

Virus-like particles (VLPs) are engineered structures comprising single or multiple self-assembling viral molecules that mimic the size and morphology of viral particles (Rawat *et al.* 2021). VLPs exhibit the advantages of non-viral genetic material, being non-infectious, and being easily prepared *via* various expression systems. VLPs mediate the immune response through antigen-presenting cell (APC) stimulation of B and T cells and also induce $CD8^+$ T cell responses to generate cellular immunity (Ewer *et al.* 2013). As an ideal antigen for vaccine production, VLPs do not rely on virus isolation and culture and are easy to manufacture in addition to having a higher safety profile (Le Thanh *et al.* 2020; Gebre *et al.* 2021). VLPs therefore offer great potential for vaccine research and development (Balke and Zeltins 2019; Nooraei *et al.* 2021). Moreover, *Flavivirus* VLPs have a unique advantage in the recognition by dendritic cells (DCs) and have been found to improve the effectiveness of vaccination (Krol *et al.* 2019). *Flavivirus* VLPs have been under development for several years, and several VLPs based on medically important viruses of the genus *Flavivirus*, including Zika virus (ZIKV), Dengue virus (DENV), Japanese encephalitis virus (JEV) and West Nile virus (WNV), have been successfully prepared using various expression systems (Salvo *et al.* 2018; Zhang *et al.* 2020).

In 2005, the International Committee on Taxonomy of Viruses (ICTV) classified TBEV into three subtypes: the European (Eu-TBEV), Siberian (Sib-TBEV), Far Eastern (FE-TBEV), and subsequently the Baikal (Bkl-TBEV) and the Himalayan (Him-TBEV) emerged later (Dai *et al.* 2018). The variation in amino acid sequences between subtypes ranges from 5–6%, and each subtype leads to varying degrees of clinical disease (Abdiyeva *et al.* 2020). Among them, FE-TBEV is the most virulent which causes severe neurological disorders, with a high mortality rate of 5–20%, and 30% of patients with FE-TBEV develop neurologic sequelae (Bogovic and Strle 2015). Vaccination against one TBEV vaccine subtype was found to be cross-protective against all TBEV subtypes, and there was no significant difference in the level of protection against different subtypes with the same vaccine (Orlinger *et al.* 2011; Fritz *et al.* 2012). The strains selected for the five existing inactivated vaccines are relatively old (Kunz *et al.* 1976; Girgsdies and Rosenkranz 1996; Kollaritsch *et al.* 2012; Prymula *et al.* 2012; Xing *et al.* 2017; Kubinski *et al.* 2020). In order to better protect animals and humans in endemic areas vulnerable to tick exposure, the FE-TBEV strain WH2012 islotead from an endemic area, was selected for the preparation of TBEV VLPs in this study.

Here, TBEV VLPs were prepared from the expression of TBEV prM-E protein through a baculovirus expression system (Fig. 1). The results demonstrated that TBEV VLPs were captured by mouse DCs after immunization and that mature DCs, supported by activated T-cells, successfully activated B-cells and generated a specific immune response with excellent immunogenicity. After three immunizations, TBEV VLPs generated specific memory T cells and a long antibody duration in mice. In conclusion, TBEV VLPs not only stimulate specific immune responses in mice but also have a high safety profile and serve as TBEV vaccine candidates, laying the foundation for the development of a novel genetically engineered vaccine against TBEV.

2. Materials and methods

2.1. Materials

Antibodies Anti-TBEV E-D III mouse serum was prepared from mice immunized with TBEV E-D III protein prepared using an *Escherichia coli*-expression system. Secondary antibodies labeled with horseradish peroxidase (HRP) or fluorescein isothiocyanate (FITC)-labeled were procured from BioWorld (USA). The goat anti-mouse IgG1 and IgG2a antibodies labeled with HRP were procured from SouthernBiotech (USA), and donkey anti-mouse IgG H&L (18 nm gold) was procured from Abcam (USA). The fluorescence-labeled monoclonal antibodies used for flow cytometry were procured from BD Biosciences (USA). The fluorescence-labeled monoclonal antibodies used for flow cytometry were procured from BD Biosciences (USA).

Stimulus *Escherichia coli*-expressed TBEV E-D III, whose amino acid sequence was consistent with that of the TBEV strain WH2012, was purified and used as a stimulus in splenocyte immunization experiments. Stimulus was added after splenocytes were cultured at 37°C for 1 h and stimulated at 37°C until the splenocyte culture was completed.

Cell culture *Spodoptera frugiperda* 9 cells (Sf9, Gibco, USA) were cultured in SFM II 900 medium (ThermoFisher Scientific, USA). Adherent-cultured Sf9 cells were incubated at 27°C in a constant temperature incubator, while suspension-cultured Sf9 cells were incubated in constant rotation on a constant temperature shaker at 120 r min^{-1}.

Mice Female BALB/c mice (6- to 8-wk-old) were procured

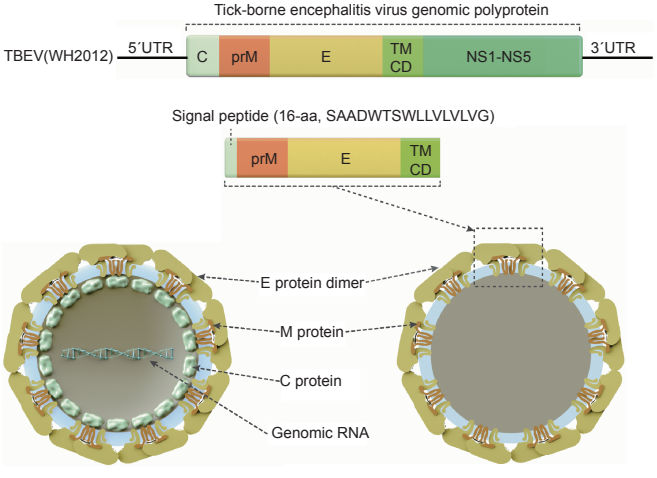


Fig. 1 The structure of tick-borne encephalitis virus (TBEV) and the strategy for constructing TBEV virus-like particles (VLPs).

from Liaoning Changsheng Biotechnology Co., Ltd. (Liaoning, China). The diet did not contain any allergens that could influence the outputs of the experiments. They were housed under standard conditions (25±3)°C, (45±5)% relative humidity, and the altering 12:12-h light-dark cycle) and fed for 7 d to acclimate before immunization and then randomly grouped at the time of immunization.

2.2. Construction of recombinant baculovirus

A gene fragment containing the TBEV prM-E (strain WH2012, Genbank: KJ755186) protein was designed. According to the SignalP-5.0 website, the prM-E signal peptide sequence of this strain was found at the C-terminus region of the C protein (16-aa, SAADWTSWLLVLVLVG). All sequences were optimized for insect cells by Sangon Biotech (Shanghai, China) and synthesized in the pUC vector.

The TBEV prM-E sequence was amplified with PCR, and the amplified target sequence was inserted into the PH (*Not*I and *Hin*dIII) and P10 (*Sma*I and *Nhe*I) promoters of the insect cell-baculovirus expression vector pFastBac Dual (Invitrogen, USA). Detailed materials and methods for homologous recombination and transfection of recombinant plasmids are described in Zhang *et al*. (2023). After 5 d of culture, when cytopathic effects (CPEs) were apparent in 50% of the cells, the supernatant was collected as the first generation (P1-generation) of recombinant baculovirus (rBV). Blind passage continued for 3 generations.

2.3. Identification of rBV with an indirect immunofluorescence assay (IFA)

Adherent-cultured Sf9 cells in excellent growth condition were evenly distributed in a 96-well plate. When the cells had reached more than 70% confluency, each well was inoculated with 10 μL of P2-generation rBV. After incubation at 27°C for 48 h, cells were fixed in 70% ethanol and stained with anti-TBEV E-D III mouse serum (1:100) as primary antibody, then stained with Evans blue (1:300) and FITC-labeled goat anti-mouse IgG (1:200). Finally, the fluorescence intensity was determined using a fluorescence microscope (Olympus Corporation, Japan).

2.4. Western blot identification of the expression form of TBEV prM-E protein

Anti-TBEV E-D III mouse serum (1:300) was used as the primary antibody, and the detailed materials and methods of WB were as described in Zhang *et al.* (2023).

2.5. Purification of TBEV VLPs

A total of 600 mL of suspension-cultured Sf9 cells infected with 6 mL of P3-generation rBV was incubated for 4 d at 27°C, with 120 r min^{-1} shaking. To remove the culture medium, cell cultures were centrifuged at 3,000×g for 15 min. The collected cells were then washed with PBS and lysed by the addition of 120 mL of cell lysis solution (1% PMSF before use). After 30 min in an ice bath, the supernatant was collected by centrifugation at 15,000×g for 15 min at 4°C. A detailed description of the methods involved in potassium tartrate-glycerol density gradient centrifugation is available in Appendix B.

The concentration of VLPs was measured using a BCA Protein Assay Kit (ThermoFisher Scientific, USA). The VLPs were then sub-packaged and stored at –80°C.

2.6. WB, electron microscopy (EM), and immune electron microscopy (IEM) analysis of TBEV VLPs

Purified TBEV VLPs were used to prepared protein samples. Anti-TBEV E-D III mouse serum (1:300) was used as the primary antibody and detailed materials and methods of WB were described in Zhang *et al.* (2023).

Twenty microliters of purified TBEV VLPs were added dropwise into the copper grid, stained and the excess liquid removed. The samples were then examined using a transmission electron microscope (H-7650, HITACHI, Japan). After twofold dilution of TBEV VLPs, 30 μL of sample was added dropwise to the copper grid and incubated for 15–20 min at room temperature. After blotting to remove the liquid, the sample was washed three times with sterile PBS. After incubation with 30 μL of 3% skimmed milk powder for 1 h at room temperature, anti-TBEV E-D III mouse serum (1:50) was added and the samples were incubated for an extra 1 h at room temperature. After 3 washes with PBS, a diluted 20× donkey anti-mouse IgG H&L (18 nm gold) secondary antibody was added, and the samples were incubated for 1 h at room temperature. After washing 3 times with PBS, the copper grid was stained and examined using electron microscopy.

2.7. Preparation of vaccines and immunizations

Antigen TBEV VLPs were diluted with sterile PBS in combination with the complex adjuvants poly(I:C) (Sigma, USA) and Montanide ISA 201VG (Seppic, France) at the volume ratio of 35:10:55 (antigen, poly(I:C), Montanide ISA 201VG) (Jin *et al.* 2022). The antigen was first mixed with poly(I:C) and then emulsified with Montanide ISA 201VG, shaken on a vortex shaker for 10 minutes, and then stood at 21°C for 1 h. The antigen TBEV VLPs were then used to immunize BALB/c mice (females, 6–8 wk). Each mouse was injected intramuscularly (IM) with 100 μL of immunogen in the hindlimb. The 100 μL immunogen included 50 ng TBEV VLPs, 200 ng poly(I:C) and 50% in weight Montanide ISA 201VG.

Mice were randomly divided into 3 groups (n=11 per group): the TBEV VLPs group (TBEV VLPs+adjuvant), the Adjuvant group (PBS+adjuvant without TBEV VLPs) and the Control group (PBS). A total of three immunizations were administered at 3-wk intervals (immunization procedures are described in Fig. 3-A).

2.8. Detection of IgG antibody titers in mouse sera using indirect ELISA

Blood was collected from the inferior ophthalmic vein at 3, 4, 7, 10, 12, 18, 22, 26, and 30 wk post-immunization (wpi), and centrifuged to obtain the sera (Dong *et al.* 2023). The levels of specific IgG antibodies in the sera of mice after immunization were analyzed by indirect enzyme-linked immunosorbent assay (ELISA) using *E. coli*-expressed recombinant TBEV E-D III protein as the coated antigen. The

detailed materials and methods about the ELISA followed those used by Zhang *et al.* (2023). The OD_{450} value was recorded immediately using a microplate reader (BioTek, USA), and the P/N (value of TBEV VLPs group/value of adjuvant group) was calculated. A P/N value≥2.1 was considered positive, at which point the dilution of the serum sample equaled the IgG antibody titer of the serum.

2.9. Flow cytometry analysis of inguinal lymphocyte activation

On day 7 (wk 1) after the first immunization, 3 mice were randomly selected from each of the three groups. The selected mice were euthanized and the inguinal lymph nodes were isolated. A lymphocyte suspension was prepared and added to two wells (5×10^5 cells/well) of a 96-well U-shaped plate (Zhang *et al.* 2022). Two different groups of antibodies were added for staining, group I: FITC-CD4, PE-CD8, PE-Cy7-CD69, PerCP-Cy5.5-CD19, and APC-CD40; group II: APC-CD80, FITC-MHC I (H-2K), PerCP-Cy5.5-MHC II (I-A/E), and PE-Cy7-CD11c, to establish single stained and unstained groups. A total of 1×10^4 cells per sample were collected using FACSCalibur (BD Biosciences, USA) and the data were analyzed using the FlowJo_V10 software.

2.10. Splenic lymphocyte proliferation assay

At wk 7 (one week after third immunization), 3 mice were randomly selected from each of the TBEV VLPs, Adjuvant, and control groups. The selected mice were euthanized, and the spleen was isolated. After the red blood cells were removed, a splenic lymphocyte suspension was prepared.

The splenic lymphocyte suspension (2.5×10^5 cells/well) was added to a 96-well plate with purified TBEV E-D III protein (0.05 μg/well) as the stimulus and incubated at 37°C and 5% CO_2 for 44 h. A total of 10 μL CCK-8 (KeyGEN Biotech, China) was then added to each well and the samples were incubated for 4 h. The OD_{450} value of the plates was read using a microplate reader (BioTek, USA), and the Prolifiteration Index (PI)=($OD_{stimulated}$– $OD_{unstimulated}$)/($OD_{unstimulated}$–OD_{blank}).

2.11. ELISpot for splenic lymphocyte differentiation (number of splenic lymphocytes secreting IFN-γ and IL-4)

Splenic lymphocyte suspension was added onto ELISpot plates at 5×10^5 cells/well together with purified TBEV E-D III protein (0.1 μg/well), and incubated at 37°C with 5% CO_2 for 36 h. ELISpot plates were processed according to the instructions of the murine IFN-γ and IL-4 ELISpot Assay Kit (Mabtech, Sweden) and then handed over to the company for collection and counting.

2.12. Meso scale discovery (MSD) multifactor assay for the detection of cytokine secretion

Splenic lymphocyte suspension (5×10^5 cells/well) and purified TBEV E-D III protein (0.1 μg/well) were added to a 96-well U-shaped plate and incubated at 37°C with 5 % CO_2 for 48 h. The culture supernatant was centrifuged at 2,500 r min^{-1} for 10 min at 4°C, then frozen at –80°C and submitted to Univ

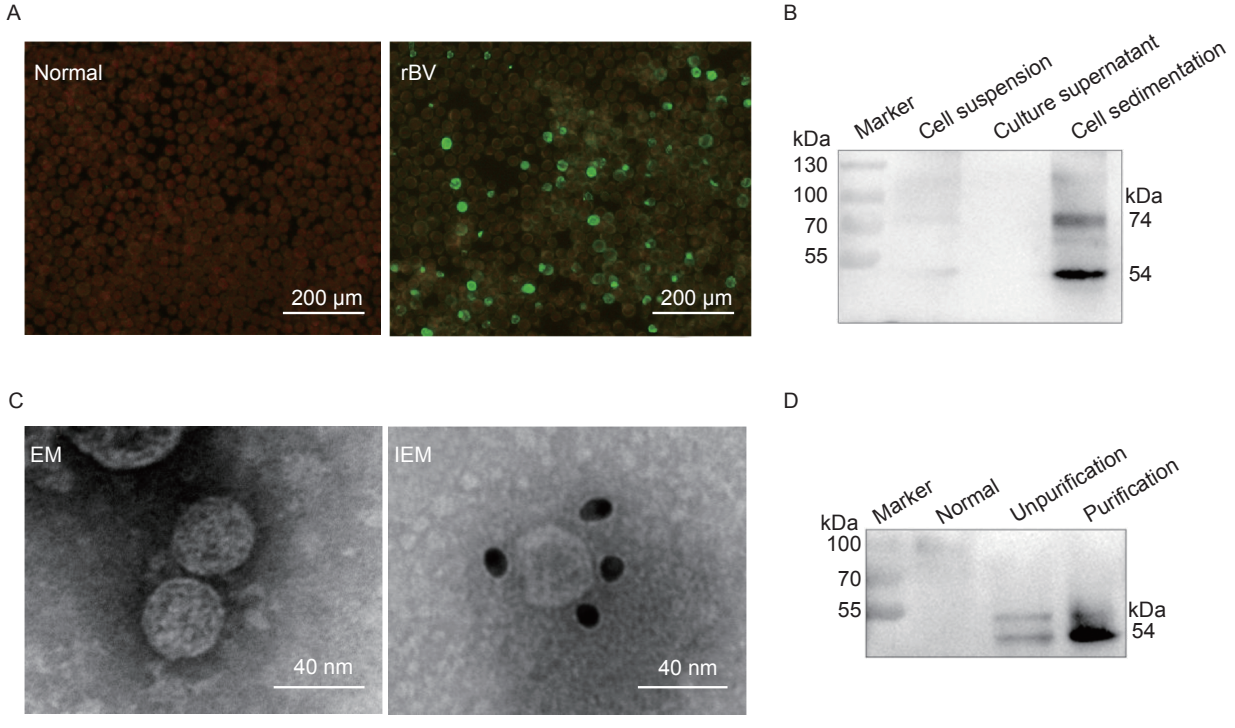


Fig. 2 Preparation and characterization of tick-borne encephalitis virus (TBEV) virus-like particles (VLPs). A, indirect immunofluorescence assay (IFA) for TBEV prM-E protein expression. B, Western blot detection of the expression form of TBEV prM-E protein. C, electron microscopy and immune electron microscopy images of purified TBEV VLPs. D, WB detection of purified TBEV VLPs. rBV, recombinant baculovirus; EM, electron microscopy, IEM, immune electron microscopy.

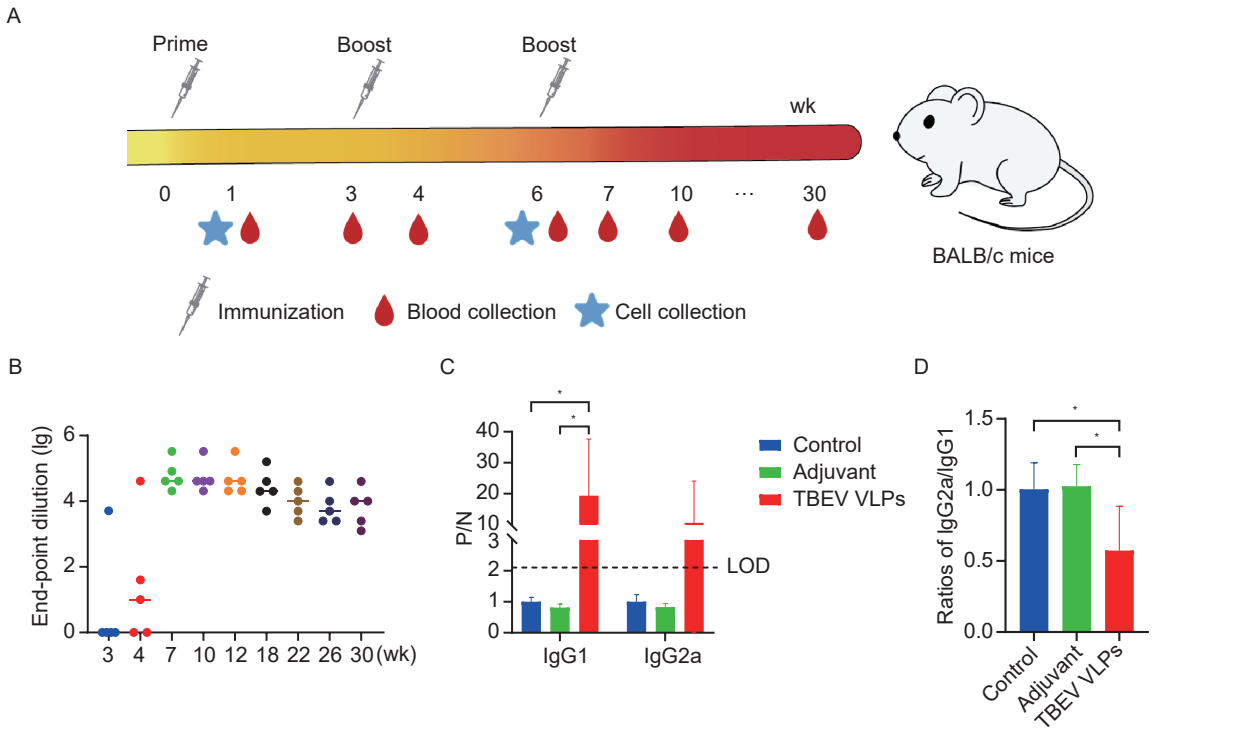


Fig. 3 The titers of specific IgG antibodies against tick-borne encephalitis virus (TBEV) in mice after immunization. Female BALB/c mice were randomized into 3 groups (n=11 per group). The TBEV virus-like particles (VLPs) and Adjuvant groups were injected (IM) with TBEV VLPs (50 μg per mouse) or PBS mixed with Poly (I:C) & Montanide ISA 201VG combination adjuvant, respectively. The control group was vaccinated (IM) with PBS. A, flowchart of the immunization procedure for BALB/c mice. Mice were immunized 3 times, with 3 wk between injections. B, TBEV-specific IgG antibody titers in serum were determined by ELISA at various time points. The x-axis represents the time points (in weeks), and the y-axis represents the serum dilution factor. The P/N ratio was calculated as the ratio of the OD_{450} value of the TBEV VLP group to that of the adjuvant control group. The endpoint titer was defined as the highest serum dilution that yielded a P/N ratio greater than 2.1. C, serum titers of IgG1 or IgG2a antibodies against TBEV were determined at wk 8 using ELISA (n=5). D, IgG2a/IgG1 ratios of the mice in each group in C were counted separately (n=5). Data are mean±SD. *, P<0.05.

(China) for MSD assay.

2.13. Flow cytometry analysis of splenic lymphocyte activation in mice

The centrifuged splenic lymphocytes (isolated in part 2.12) were divided into two groups (5×10^5 cells per sample) and stained with different antibodies: group 1: FITC-CD4, PE-CD8, PerCP-Cy5.5-CD62L and APC- CD44; group 2: FITC-CD4, PE-CD8, PE-Cy7-CD69, PerCP-Cy5.5-CD19 and APC-CD40. A total of 1×10^4 cells per sample were collected using FACSCalibur (BD Biosciences, USA) and were analyzed for the presence of a fluorescence signal.

2.14. Statistical analyses

All experiments were replicated 3 or more times, and statistical analyses of experimental results, expressed as mean±SD, were performed with Student's t-test using the GraphPad 8.4.3 software. A P-value of ≤0.05 was considered significantly different.

3. Results

3.1. Preparation and characterization of TBEV VLPs

The C-terminal transmembrane structural domain of C protein plays a role as an additional anchor point and signal peptide for the prM protein, which is beneficial for the expression of prM protein (Blazevic *et al.* 2016). As shown in Fig. 1, the 16 amino acid sequence at the C-terminus was used as the signal peptide. Moreover, an insect cell-baculovirus expression system, which was easy to scale up and relatively inexpensive, was chosen to express the TBEV prM-E protein. Compared to normal cells, the recombinant baculovirus (rBV)-infected Sf9 cells developed obvious CPEs such as swelling, rounding and massive shedding (Appendix A). TBEV prM-E protein expression was assessed using an indirect immunofluorescence assay (IFA) with TBEV E-D III antibody as the primary antibody. The rBV-infected Sf9 cells showed obvious green fluorescence under fluorescence microscopy, while normal cells showed no green fluorescence, indicating that rBV-infected Sf9 cells were capable of expressing TBEV E protein (Fig. 2-A). The rBV-infected cell suspensions, culture supernatants and cell sediment suspensions were examined with WB to analyze the expression form of the TBEV prM-E protein. The specific protein was not detected in the rBV culture supernatant, whereas 74 and 54 kDa specific bands appeared in the rBV cell sediment suspension (Fig. 2-B). The Editseq software predicted the TBEV prM-E and E proteins were approximately 74 and 54 kDa, respectively. TBEV has only one ORF, and different proteins are cleaved by the

enzyme during the viral particle assembly process. This therefore explains the two bands (74 and 54 kDa) detected in the rBV cell sediment suspension (Fuzik *et al.* 2018). In conclusion, rBV-infected Sf9 cells expressed TBEV prM-E protein mainly in the cytoplasm, and the cleaved TBEV E protein was detected in the rBV cell sediment suspension. The cleaved TBEV E protein has the potential to generate mature TBEV VLPs.

3.2. Purification and characterization of TBEV VLPs

The TBEV VLPs were obtained by density gradient centrifugation following the procedure described in Appendix B. After the lysis of the cells with cell lysis solution, cell debris was removed by high-speed centrifugation. The supernatant after centrifugation was ultracentrifuged, and the proteins were aggregated at the bottom of the tube with a burnt yellow translucent appearance Appendix B-a. After adding different densities of potassium tartrate-glycerol sequentially in a 15 mL centrifuge tube, there was obvious stratification between the different densities. After adding the preliminary purified protein solution, the protein solution was suspended on the gradient liquid surface Appendix B-b. After density gradient centrifugation, the protein was divided into one layer, approximately between 15–30% of the potassium tartrate-glycerol density gradient, in the form of a pale yellow solid Appendix B-d. The precipitate was resuspended with approximately 6 mL of sterile PBS to prepare the VLPs and the protein concentration was measured at 8 mg mL^{-1} by BCA. The VLPs contained the fully cleaved TBEV E protein (Fig. 2-D). The VLPs exhibited spherical morphology, with a diameter of ~40–60 nm (Fig. 2-C); this is similar in morphology and structure to TBEV (Fuzik *et al.* 2018). Furthermore, the E protein of the VLPs was verified with immunoelectron microscopy, and the gold particles and the gold particles were attached to the surface of the VLPs. Together, these results suggested the TBEV VLPs were successfully prepared.

3.3. TBEV VLPs induce the production of IgG antibodies against TBEV in mice

To evaluate the effect of immunization with the TBEV VLPs, BALB/c mice were immunized following the described immunization procedure (Fig. 3-A). Mice did not show any abnormalities or adverse effects after immunization. Neutralizing antibodies are the key element to prevent virus infection, whereas the TBEV culture and animal infection experiment require biosafety level 3 (BSL-3) and ABSL-3 laboratory. TBEV E-D III contains a large number of neutralizing antibody epitopes. To evaluate the immune effect of TBEV VLPs, we tested IgG antibodies against the TBEV E-D III region by an indirect enzyme-linked immunosorbent assay (ELISA) (Fig. 3-B), using the prokaryotic-expressed TBEV E-D III protein as the coated antigen. IgG antibodies against TBEV were detected in most mice (average value 1:10) at wk 4. The titers increase significantly at wk 7, up to $1:10^{5.5}$ (average value $1:10^{4.6}$) and began to decrease slowly at wk 18 remaining at $1:10^{4}$ (average value) up to 30 wk of detection.

The titers of IgG1 and IgG2a antibodies against TBEV were assessed using indirect ELISA at wk 8 following immunization. We found that IgG1 antibodies were considerably elevated in the TBEV VLPs group compared with the other two groups (Fig. 3-C), and the value of the IgG2a/IgG1 ratio was less than 1 and significantly lower than in either of the two controls (Fig. 3-D), indicating that mice immunized with TBEV VLPs produced a Th2-type biased immune response.

3.4. DCs, B-cell and T-cell activation following immunization

The experiments described above verified the immune effect of TBEV VLPs from the humoral perspective, and we next analyzed the effect of TBEV VLPs on immune cells in mice. We first investigated the activation effect of TBEV VLPs on murine DCs, T-cells, and B-cells. Inguinal lymphocytes were isolated and measured using flow cytometry on wk 1 after the first immunization. The $CD11c^+$ $CD80^+$, $CD11c^+$ MHC I^+ and $CD11c^+$ MHC II^+ double-positive cells in the TBEV VLPs group were more than that in the other two groups (Fig. 4), which indicated that the DCs were activated in the TEBV VLPs group following the first immunization, and the MHC class I and class II pathways were initiated. A considerable difference was identified neither in $CD4^+$ $CD69^+$ nor in $CD8^+$ $CD69^+$ double-positive cells in the TBEV VLPs group compared to the other groups Appendix C, implying undetectable T-cell activation following the first immunization. $CD19^+$ $CD40^+$ double-positive cells in the TBEV VLPs group were significantly more frequent than in the Control group, and $CD19^+$ $CD69^+$ were also substantially greater than in the other two groups (Fig. 5), reflecting that B-cell activation had occurred following immunization.

We also investigated whether T-cells in the splenic lymphocytes were activated on the 7th day following the 3rd immunization. The flow cytometric results revealed that $CD4^+$ $CD69^+$ was substantially more in the TBEV VLPs group than the Adjuvant group (Fig. 6), and no significant difference in $CD8^+$ $CD69^+$ double positive cells were detected in the TBEV VLPs group compared to the other groups Appendix D, showing that the TBEV VLPs effectively activated DCs, $CD4^+$ T-cells, and B-cells to induce immune responses in mice.

3.5. Splenocyte differentiation and proliferation after *in vitro* stimulation

Mature lymphocytes depend on antigenic stimulation to differentiate, proliferate, and perform immune functions. The spleen is the largest peripheral immune organ, and the differentiation and proliferation of splenic lymphocytes under the stimulation of TBEV antigens following the 3rd immunization is also an essential indicator to assess the effect of vaccination with the vaccine. On the 7th day after the 3rd and final injection, splenic lymphocytes were isolated from mice, and the proliferation of the splenic lymphocytes was investigated with CCK-8 assays after stimulation with the TBEV E-D III protein *in vitro*. The splenic lymphocytes in the TBEV VLPs group had proliferated significantly more than those in the other two groups (Fig. 7-A), which demonstrated

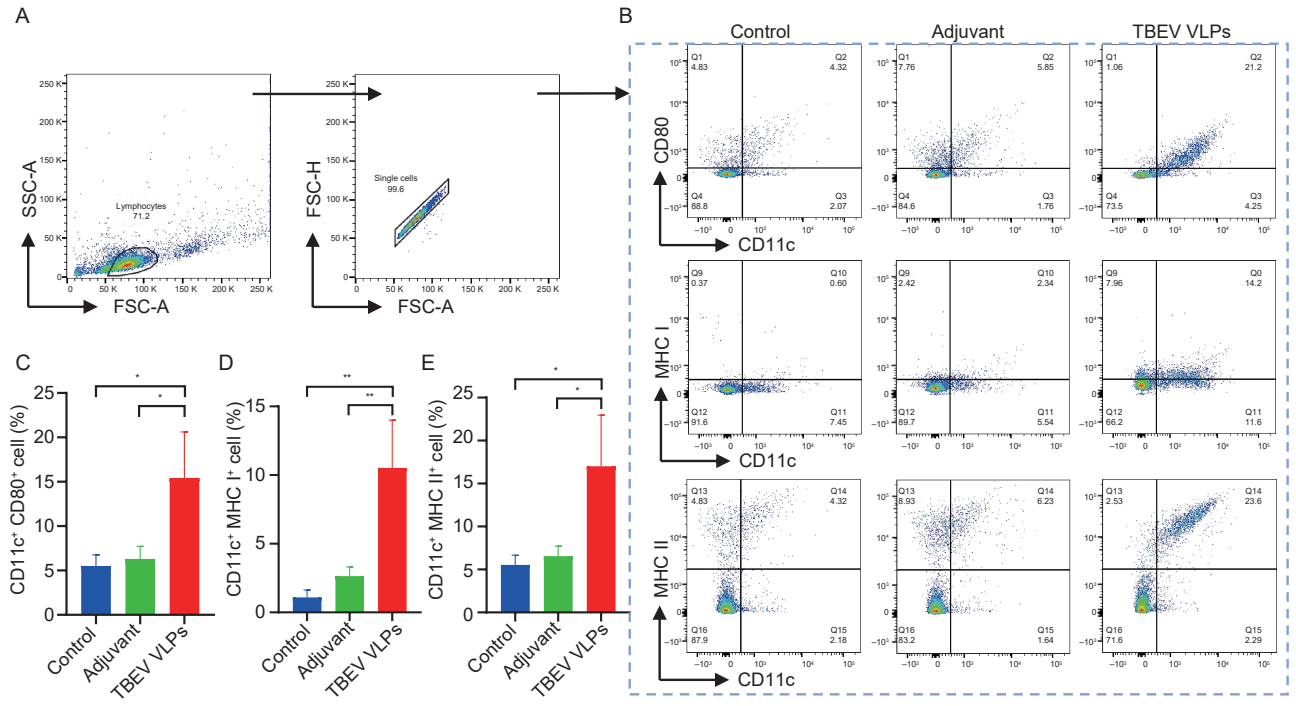


Fig. 4 Early activation of DCs in the inguinal lymph nodes of mice on the 7th day after the 1st immunization (*n*=3 per group). A, gating strategy for flow cytometric scatter plots to analyze the activation of the dendritic cells (DCs) in lymph nodes after the 1st immunization. B, representative flow plots for CD80-CD11c, MHC I-CD11c, and MHC II-CD11c lymphocytes. C–E, proportion of CD80$^+$ CD11c$^+$, MHC I$^+$ CD11c$^+$, and MHC II$^+$ CD11c$^+$ double-positive lymphocytes. Data are mean±SD. *, P<0.05, **, P<0.01.

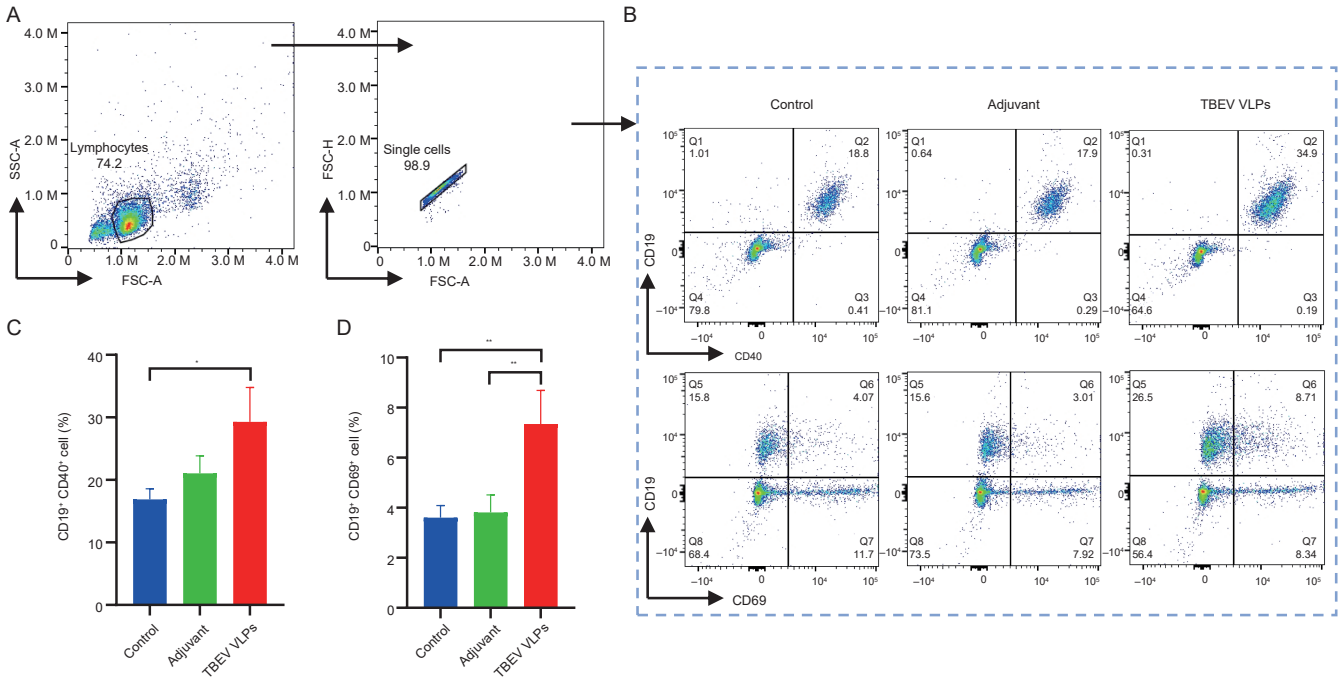


Fig. 5 Early activation of B-cells in the inguinal lymph nodes of mice on the 7th after the 1st immunization (*n*=3 per group). A, gating strategy for flow cytometric scatter plots to analyze the B-cell activation in lymph nodes after the 1st immunization. B, representative flow plots for CD19-CD40 and CD19-CD69 lymphocytes. C and D, proportion of CD19$^+$ CD40$^+$ and CD19$^+$ CD69$^+$ double-positive lymphocytes. Data are mean±SD. *, P<0.05, **, P<0.01.

that the splenic lymphocytes of mice immunized with TBEV VLPs specifically recognized the antigen and generated an adaptive immune response when stimulated with the TBEV antigenic protein.

As detected using enzyme-linked immunospot assay (ELISpot), the number of splenic lymphocytes secreting

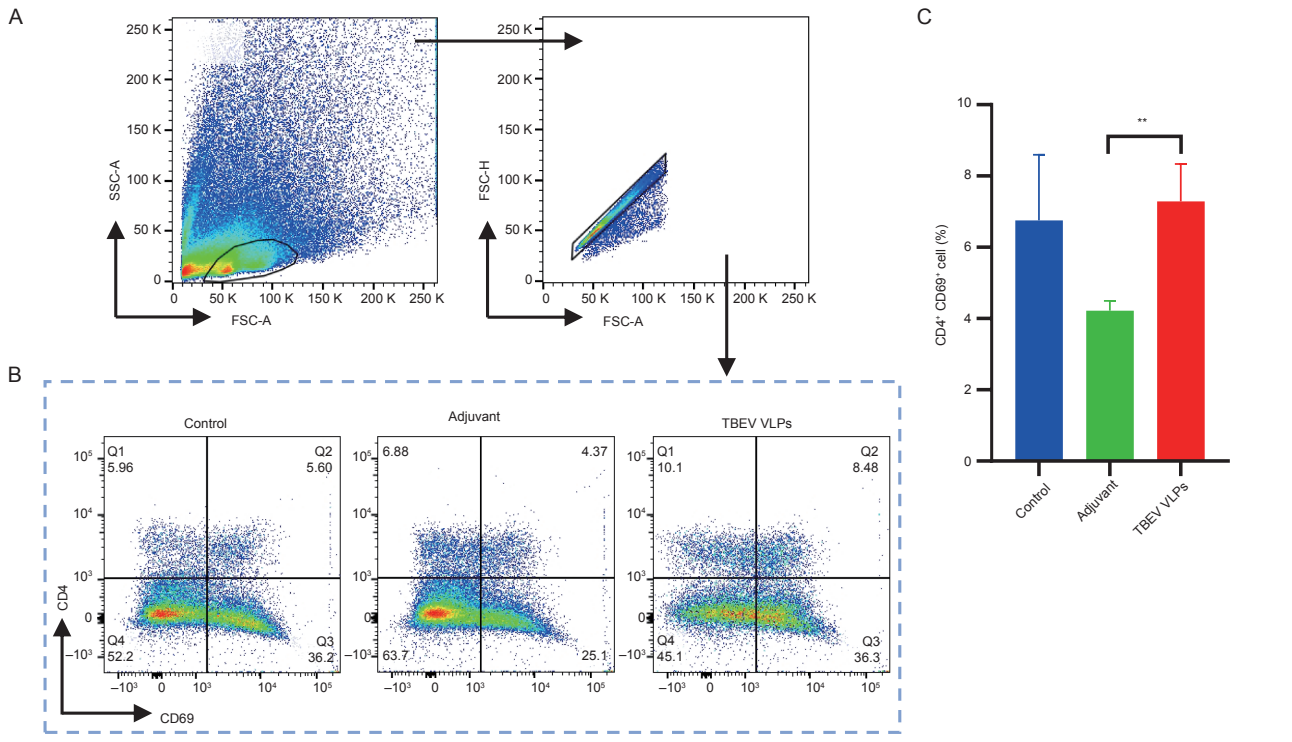


Fig. 6 Activation of T-cells in the inguinal lymph nodes of mice on the 7th after the 3rd immunization (*n*=3 per group). A, gating strategy for flow cytometric scatter plots to analyze the activation of the T-cells in the spleen after the 3rd immunization. B, representative flow plots for CD4-CD69 lymphocytes. C, proportion of $CD4^+$ $CD69^+$ double-positive lymphocytes. Data are mean±SD. **, $P<0.01$.

interferon-γ (IFN-γ) was higher in the TBEV VLPs group than in the Adjuvant group. The number of splenic lymphocytes secreting interleukin 4 (IL-4) was considerably higher than in the other groups (Fig. 7-B). IFN-γ is the major cytokine in the Th1-type immune response, and IL-4 is that of the Th2-type immune response. After mice were immunized with TBEV VLPs, splenic lymphocytes secreting IFN-γ and IL-4, both increased significantly. However, the proliferation of IL-4-secreting lymphocytes was more pronounced (Fig. 7-B). The above results indicated that after multiple immunizations of mice with TBEV VLPs, splenic lymphocytes proliferated and differentiated *in vitro* when stimulated with TBEV antigen, generating Th1 and relatively more Th2 cells, which was consistent with the results from the IgG subtype assay in mice (Fig. 3-D).

3.6. Increased cytokine secretion in mice after *in vitro* stimulation

The secretion of cytokines after differentiation and proliferation of splenic lymphocytes is also one of the indicators that an immune response has occurred. Splenic lymphocytes from mice were extracted on the 7th day after the 3rd immunization and were stimulated and cultured in vitro for 48 h. Cell culture supernatants were collected. The cytokine secretion was assessed using, and cytokine secretion was assessed using a meso scale discovery (MSD) multifactor assay (Fig. 7-C and D). The results showed that splenic lymphocytes in the TBEV VLPs group of mice secreted significantly more IL-5 and IL-6 than those in the adjuvant group. It has been previously reported that IFN-γ, IL-12p70, THF-α, IL-2, and KC/GRO are Th1-type cytokines, while IL-4, IL-5, IL-6, IL-10, and IL-1β are Th2-type cytokines (Zhang *et al.* 2023). Therefore, our results indicated that the mice immunized with TBEV VLPs markedly elicited the Th2-type immune responses, consistent with the results from the mouse IgG subtype assay and ELISpot (Figs. 3-D and 7-B).

3.7. Mouse spleen produces memory T-cells after three immunizations

Immune memory is the basis and prerequisite for vaccine immunity. The prolonged survival of memory T-cells (T_M) in the body would rapidly mediate the production of a protective immune response when stimulated by a particular antigen again (Cox and Brokstad 2020). Central memory T-cells (T_{CM}) secrete abundant CD62L after antigen stimulation, and they divide and proliferate rapidly, migrate to effector sites, and play a crucial part in the secondary response. On the contrary, effector memory T-cells (T_{EM}) possess low CD62L secretion and weak proliferative capacity, respond rapidly to secondary responses, produce direct cell lysis activity, and to produce cytokines and eliminate infected cells rapidly (Cuddapah *et al.* 2010). On the seventh day after the 3rd immunization, the production of T_M from the splenic $CD4^+$ and $CD8^+$ subpopulations of mice was analyzed using flow cytometry (Fig. 8). The results showed that $CD4^+$/$CD44^+CD62L^+$ double positive cells (T_{CM}, Q2) was noticeably more in the TBEV VLPs group than in the other groups. The $CD4^+$/$CD44^+CD62L^-$ cells (T_{EM}, Q1) were also clearly

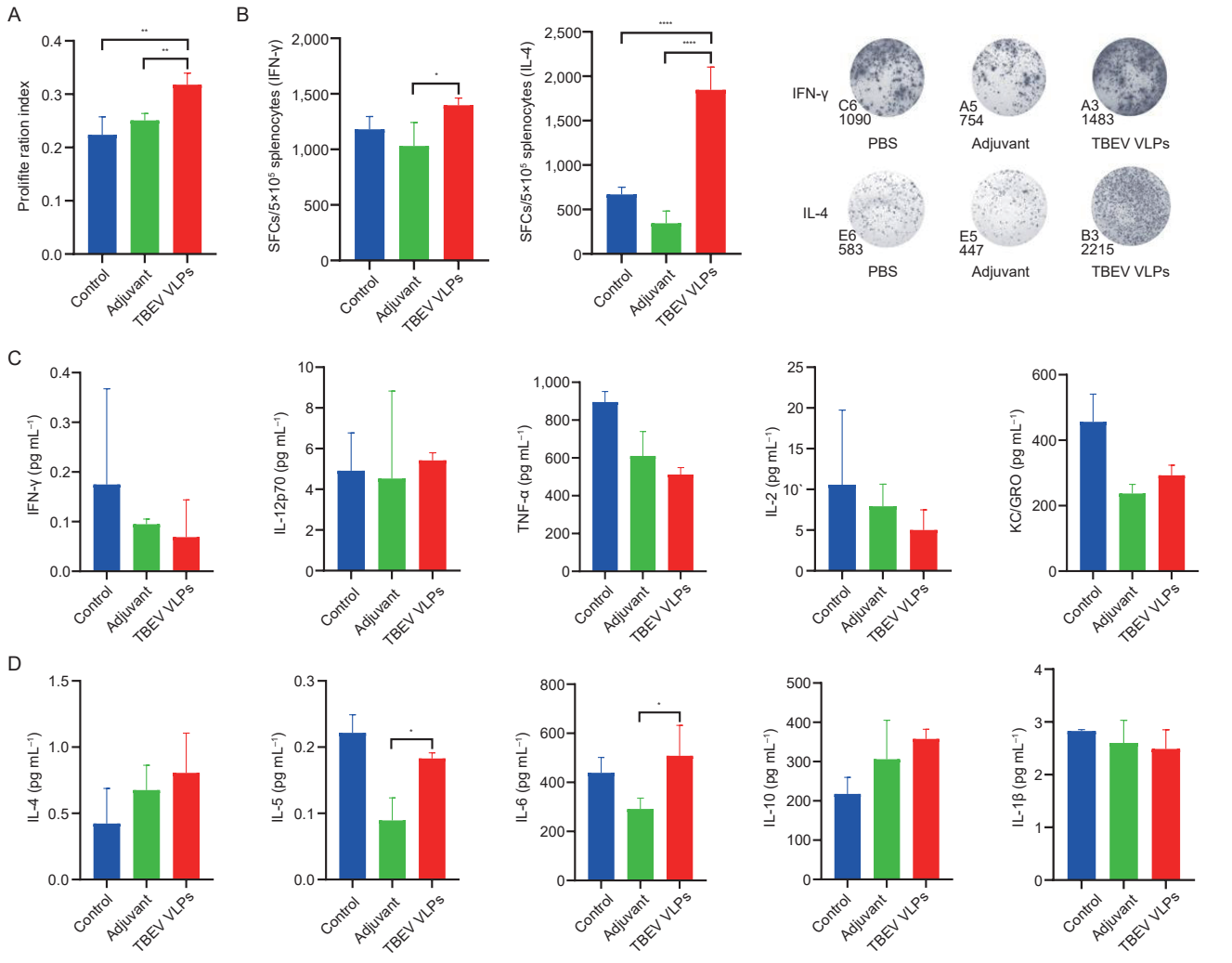


Fig. 7 Systemic cellular immunity analysis in the inguinal lymph nodes of mice on the 7th after the 3rd immunization (*n*=3 per group). A, detection of the proliferative index *via* CCK-8 assay. B, statistical data of splenic lymphocytes secreting IFN-γ or IL-4 and the ELISpot assay images. C and D, Th1-type cytokines C and Th2-type cytokines D in splenic lymphocyte culture supernatants were quantified using a meso scale discovery (MSD) multifactor assay. TBEV, tick-borne encephalitis virus; VLPs, virus-like particles. Data are mean±SD. *, $P<0.05$, **, $P<0.01$; ****, $P<0.0001$.

higher than in the Control or Adjuvant groups. Furthermore, $CD8^+/CD44^+CD62L^+$ double positive cells (T_{CM}, Q2) were substantially higher in the TBEV VLPs group than in the other groups, and $CD8^+/CD44^+CD62L^-$ cells (T_{EM}, Q1) were also clearly more than in the Adjuvant group. TBEV VLPs can produce immune memory in mice after the 3rd immunization.

4. Discussion

TBEV is a positive-sense single-stranded RNA virus belonging to the *Flavivirus* genus of the *Flaviviridae* family. The genome is approximately 11,000 nt in length, containing an open reading frame, which expresses three structural proteins (C, M, and E) and seven non-structural proteins (Fuzik *et al.* 2018). The mature virion comprises 90 dimers of E and M proteins (Chong *et al.* 2019). The M protein, which is anchored to the lipid envelope by two transmembrane domains, interacts with the transmembrane domain of the E protein in the mature particle to assist in the correct folding of the E protein (Luo *et al.* 2015). The E protein plays an essential role in immunization and prevention, as this envelope protein interacts with specific cell surface receptors to induce the fusion of the viral envelope with the host cell membrane when the virus enters the cell. During *Flavivirus* assembly, the prM-E protein is cleaved by host cell furin protease to produce pr fragments and the M-E protein. The host cell signal peptidase I cleaves the M-E protein into the M and E proteins (Krol *et al.* 2019).

In this study, the prM-E protein of TBEV was expressed using an insect cell-baculovirus expression system, in which signal peptidase from Sf9 cells could recognize signal sequences of prM and E proteins. Therefore, two types of proteins were produced during the expression of TBEV prM-E: the prM-E protein (the protein at 74 kDa in Fig. 2-B) and the M and E protein dimers (the E protein at 54 kDa was detected in Fig. 2-B). Since it has been demonstrated that only mature VLPs have viral-like properties (Krol *et al.* 2019), we purified the prepared protein solution with density gradient centrifugation. As shown in Fig. 2-D, the 74 kDa proteins

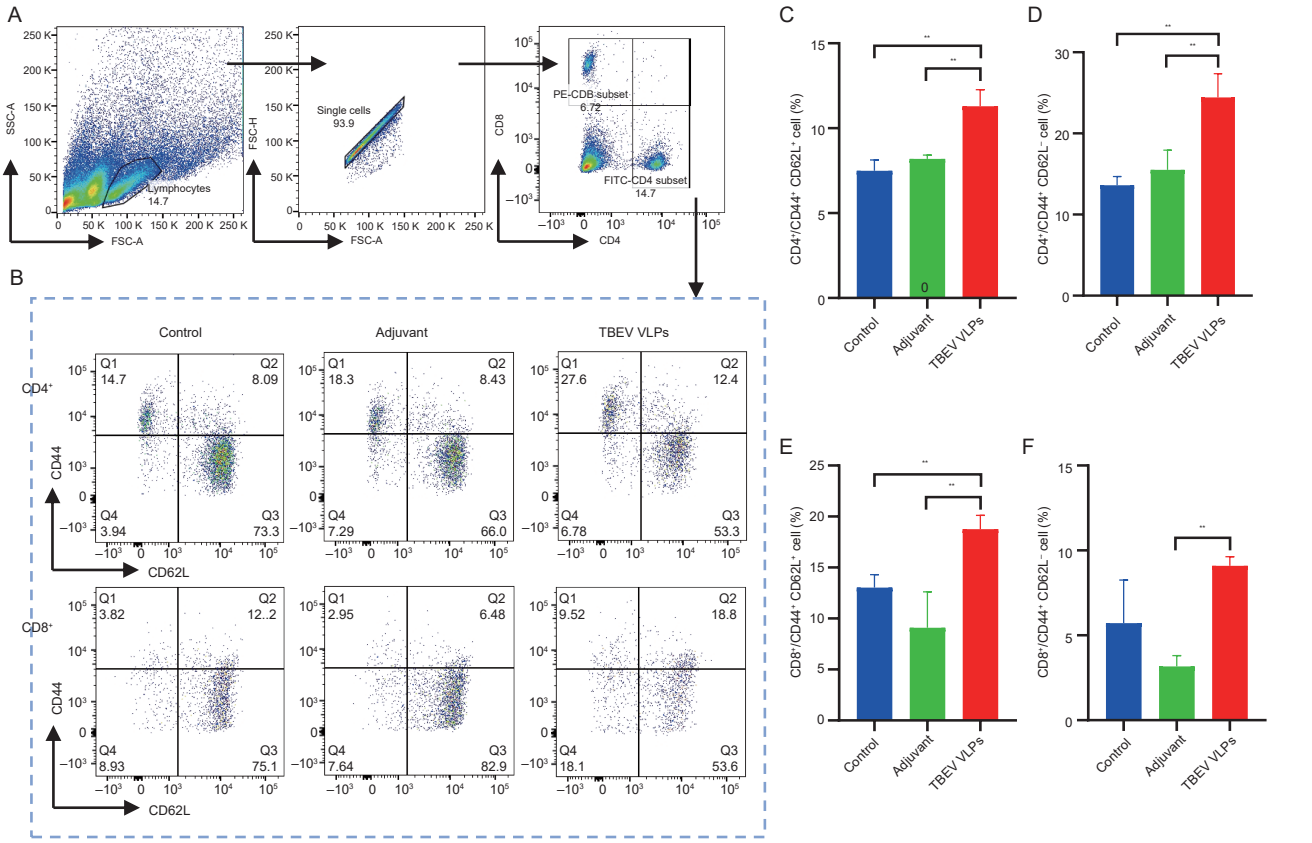


Fig. 8 Memory T-cell analysis in the inguinal lymph nodes of mice on the 7th after the 3rd immunization (*n*=3 per group). A, gating strategy for flow cytometric scatter plots to analyze the production of memory T-cells in the spleen after three immunizations. B, representative flow plots for $CD4^+/CD44^+CD62L^+$, $CD4^+/CD44^+CD62L^-$, $CD8^+/CD44^+CD62L^+$ and $CD8^+/CD44^+CD62L^-$ lymphocytes. C–F, proportion of $CD4^+/CD44^+CD62L^+$, $CD4^+/CD44^+CD62L^-$, $CD8^+/CD44^+CD62L^+$ and $CD8^+/CD44^+CD62L^-$ lymphocytes. Data are mean±SD. **, $P<0.01$.

were almost absent in the supernatant from the lysed cells, probably because most of the uncleaved proteins adhered to the cell or organelle membrane and were removed with the sediment after centrifugation. The EM results in Fig. 2-C verified that the purified protein solution contained a large number of mature TBEV VLPs. In summary, mature TBEV VLPs could be assembled by expressing TBEV prM-E through the insect cell-baculovirus expression system, and purer mature TBEV VLPs were obtained after potassium tartrate-glycerol density gradient centrifugation.

Activation of DCs and B-cells was detected in the inguinal lymph nodes one week after the first immunization (Figs. 4 and 5). We presumed that DCs captured TBEV VLPs after the immunization of mice; the activated DCs processed the antigen and presented MHC class I and II molecules to T-cells, and the T-cells were activated with the synergistic stimulation of CD80. However, our study showed no T-cell responses in early immunization Appendix C. Although B-cell response to most antigens required T-cells-helpers, we detected B-cell activation without T-cell activation (Fig. 5). This may be attributed to the production of low-affinity IgM antibodies in mice after stimulation, which was consistent with what we detected after the 1st immunization (Fig. 3-B). Antibody production requires the involvement of T-cells for most antigens, as well as Th-cells, to cause B-cells proliferation, differentiation, antibody production, and antibody class switching and affinity maturation. Fortunately, activation of $CD4^+$ T-cells was detected in the spleen after the third immunization (Fig. 6), and no specific $CD8^+$ T-cells were detected, probably due to the small number of cell samples. $CD4^+$ T-cells provided "helper" signals that regulated B-cell differentiation and selection, effectively promoting the production of humoral immunity (Kent *et al.* 2022). B-cells were activated with the help of $CD4^+$ T-cells (Fig. 5), consistent with the result detected after the 3rd immunization (Fig. 3-B).

Robust antibody response is critical for a TBEV vaccine because humoral immunity is essential for preventing *Flavivirus* infection (Mansfield *et al.* 2011). Viral culture and animal infection experiments for TBEV require BSL-3 and ABSL-3 laboratories. The antigenic epitopes of the TBEV E protein domain III (E-D III) have the highest neutralizing activity of the epitopes, and the humoral immune response predominantly produces TBEV E-D III-specific antibodies (Pierson *et al.* 2008; Zlatkovic *et al.* 2011). Consequently, after three immunizations with TBEV VLPs, the mice developed a long-term, high-level humoral immune response against TBEV (Fig. 3-B). Moreover, memory T-cells maintain in the body for an extended period and effectively mediate long-term protective immune responses.

The production of memory T cells after the 3rd immunization was monitored in the splenic lymphocytes of mice (Fig. 8). In summary, following three immunizations with TBEV VLPs, mice developed specific immune memory.

5. Conclusion

TBEV VLPs prepared by the expression of the prM-E protein as a VLP vaccine with excellent immunogenicity generate long-term antibody persistence against TBE in mice. This VLP-based vaccine provides a technical reserve for the prevention and control of TBEV and offers a strategy for the development of other virus subunit vaccines.

Acknowledgements

This work was supported by the National Key Research and Development Program of China (2021YFC2600202) and the Fundamental Research Funds for the Central Universities, China (2132020KJC016).

Declaration of competing interest

The authors declare that they have no conflict of interest.

Declaration of generative AI and AI-assisted technologies in the writing process

The authors declare that they did not use AI in the preparation and writing of this manuscript.

Ethical approval

This study was performed in strict accordance with the recommendations in the Guide for the Care and Use of Laboratory Animals of the Ministry of Science and Technology of the People's Republic of China. All procedures complied with the Jilin University Animal Ethics Committee (SY202207009).

Appendices associated with this study are available at https://doi.org/10.1016/j.jia.2024.09.024

References

Abdiyeva K, Turebekov N, Yegemberdiyeva R, Dmitrovskiy A, Yeraliyeva L, Shapiyeva Z, Nurmakhanov T, Sansyzbayev Y, Froeschl G, Hoelscher M, Zinner J, Essbauer S, Frey S. 2020. Vectors, molecular epidemiology and phylogeny of TBEV in Kazakhstan and central Asia. *Parasites & Vectors*, **13**, 504.

Balke I, Zeltins A. 2019. Use of plant viruses and virus-like particles for the creation of novel vaccines. *Advanced Drug Delivery Reviews*, **145**, 119–129.

Blazevic J, Rouha H, Bradt V, Heinz F X, Stiasny K. 2016. Membrane anchors of the structural flavivirus proteins and their role in virus assembly. *Journal of Virology*, **90**, 6365–6378.

Bogovic P, Strle F. 2015. Tick-borne encephalitis: A review of epidemiology, clinical characteristics, and management. *World Journal of Clinical Cases*, **3**, 430–441.

Bungener L, Geeraedts F, Ter Veer W, Medema J, Wilschut J, Huckriede A. 2008. Alum boosts TH2-type antibody responses to whole-inactivated virus influenza vaccine in mice but does not confer superior protection. *Vaccine*, **26**, 2350–2359.

Chong H Y, Leow C Y, Abdul Majeed A B, Leow C H. 2019. Flavivirus infection — A review of immunopathogenesis, immunological response, and immunodiagnosis. *Virus Research*, **274**, 197770.

Cox R J, Brokstad K A. 2020. Not just antibodies: B cells and T cells mediate immunity to COVID-19. *Nature Reviews Immunology*, **20**, 581–582.

Cuddapah S, Barski A, Zhao K. 2010. Epigenomics of T cell activation, differentiation, and memory. *Current Opinion in Immunology*, **22**, 341–347.

Dai X, Shang G, Lu S, Yang J, Xu J. 2018. A new subtype of eastern tick-borne encephalitis virus discovered in Qinghai-Tibet Plateau, China. *Emerging Microbes & Infections*, **7**, 74.

Demina T V, Dzhioev Y P, Verkhozina M M, Kozlova I V, Tkachev S E, Plyusnin A, Doroshchenko E K, Lisak O V, Zlobin V I. 2010. Genotyping and characterization of the geographical distribution of tick-borne encephalitis virus variants with a set of molecular probes. *Journal of Medical Virology*, **82**, 965–976.

Dong L, Xiao J, Liu S, Deng G, Liao Y, Chu B, Zhao X, Song B L, Luo J. 2023. Lysosomal cholesterol accumulation is commonly found in most peroxisomal disorders and reversed by 2-hydroxypropyl-β-cyclodextrin. *Science China-Life Sciences*, **66**, 1786–1799.

Donoso Mantke O, Escadafal C, Niedrig M, Pfeffer M, Working Group For Tick-Borne Encephalitis Virus C. 2011. Tick-borne encephalitis in Europe, 2007 to 2009. *Eurosurveillance*, **16**, 19976.

Esser H J, Lim S M, de Vries A, Sprong H, Dekker D J, Pascoe E L, Bakker J W, Suin V, Franz E, Martina B E E, Koenraadt C J M. 2022. Continued circulation of tick-borne encephalitis virus variants and detection of novel transmission foci, the Netherlands. *Emerging Infectious Diseases*, **28**, 2416–2424.

Ewer K J, O'Hara G A, Duncan C J, Collins K A, Sheehy S H, Reyes-Sandoval A, Goodman A L, Edwards N J, Elias S C, Halstead F D, Longley R J, Rowland R, Poulton I D, Draper S J, Blagborough A M, Berrie E, Moyle S, Williams N, Siani L, Folgori A, *et al.* 2013. Protective $CD8^+$ T-cell immunity to human malaria induced by chimpanzee adenovirus-MVA immunisation. *Nature Communications*, **4**, 2836.

Fares W, Dachraoui K, Cherni S, Barhoumi W, Slimane T B, Younsi H, Zhioua E. 2021. Tick-borne encephalitis virus in Ixodes ricinus (Acari: Ixodidae) ticks, Tunisia. *Ticks and Tick-borne Diseases*, **12**, 101606.

Fritz R, Orlinger K K, Hofmeister Y, Janecki K, Traweger A, Perez-Burgos L, Barrett P N, Kreil T R. 2012. Quantitative comparison of the cross-protection induced by tick-borne encephalitis virus vaccines based on European and Far Eastern virus subtypes. *Vaccine*, **30**, 1165–1169.

Fuzik T, Formanova P, Ruzek D, Yoshii K, Niedrig M, Plevka P. 2018. Structure of tick-borne encephalitis virus and its neutralization by a monoclonal antibody. *Nature Communications*, **9**, 436.

Gebre M S, Brito L A, Tostanoski L H, Edwards D K, Carfi A, Barouch D H. 2021. Novel approaches for vaccine development. *Cell*, **184**, 1589–1603.

Girgsdies O E, Rosenkranz G. 1996. Tick-borne encephalitis: Development of a paediatric vaccine. A controlled, randomized, double-blind and multicentre study. *Vaccine*, **14**, 1421–1428.

Jin H, Bai Y, Wang J, Jiao C, Liu D, Zhang M, Li E, Huang P, Gong Z, Song Y, Xu S, Feng N, Zhao Y, Wang T, Li N, Gao Y, Yang S, Zhang H, Li Y, Xia X, *et al.* 2022. A bacterium-like particle vaccine displaying Zika virus prM-E induces systemic immune responses in mice. *Transboundary and Emerging Diseases*, **69**, e2516–e2529.

Kent S J, Khoury D S, Reynaldi A, Juno J A, Wheatley A K, Stadler E, John Wherry E, Triccas J, Sasson S C, Cromer D, Davenport M P. 2022. Disentangling the relative importance of T cell responses in COVID-19: Leading actors or supporting cast? *Nature Reviews Immunology*, **22**, 387–397.

Kollaritsch H, Paulke-Korinek M, Holzmann H, Hombach J, Bjorvatn B, Barrett A. 2012. Vaccines and vaccination against tick-borne encephalitis. *Expert Review of Vaccines*, **11**, 1103–1119.

Krol E, Brzuska G, Szewczyk B. 2019. Production and biomedical application of flavivirus-like particles. *Trends in Biotechnology*, **37**, 1202–1216.

Kubinski M, Beicht J, Gerlach T, Volz A, Sutter G, Rimmelzwaan G F. 2020. Tick-borne encephalitis virus: A quest for better vaccines against a virus on the rise. *Vaccines* (Basel), **8**, 451.

Kunz C, Hofmann H, Stary A. 1976. Feldversuche mit einem Impfstoff gegen die Frühsommer-Meningoenzephalitis (FSME) (Field studies with a new tick-borne encephalitis (TBE) vaccine). *Medizinische Mikrobiologie und Parasitologie*, **234**, 141–144.

Li J X, Wu S P, Guo X L, Tang R, Huang B Y, Chen X Q, Chen Y, Hou L

H, Liu J X, Zhong J, Pan H X, Shi F J, Xu X Y, Li Z P, Zhang X Y, Cui L B, Tan W J, Chen W, Zhu F C. 2022. Safety and immunogenicity of heterologous boost immunisation with an orally administered aerosolised Ad5-nCoV after two-dose priming with an inactivated SARS-CoV-2 vaccine in Chinese adults: A randomised, open-label, single-centre trial. *Lancet Respiratory Medicine*, **10**, 739–748.

Lim J M E, Hang S K, Hariharaputran S, Chia A, Tan N, Lee E S, Chng E, Lim P L, Young B E, Lye D C, Le Bert N, Bertoletti A, Tan A T. 2022. A comparative characterization of SARS-CoV-2-specific T cells induced by mRNA or inactive virus COVID-19 vaccines. *Cell Reports Medicine*, **3**, 100793.

Liu Y, Zeng Q, Deng C, Li M, Li L, Liu D, Liu M, Ruan X, Mei J, Mo R, Zhou Q, Liu M, Peng S, Wang J, Zhang H, Xiao H. 2022. Robust induction of B cell and T cell responses by a third dose of inactivated SARS-CoV-2 vaccine. *Cell Discovery*, **8**, 10.

Loew-Baselli A, Konior R, Pavlova B G, Fritsch S, Poellabauer E, Maritsch F, Harmacek P, Krammer M, Barrett P N, Ehrlich H J. 2006. Safety and immunogenicity of the modified adult tick-borne encephalitis vaccine FSME-IMMUN: Results of two large phase 3 clinical studies. *Vaccine*, **24**, 5256–5263.

Luo Y, Guo X, Yan H, Fang D, Zeng G, Zhou J, Jiang L. 2015. Comprehensive mapping infection-enhancing epitopes of dengue pr protein using polyclonal antibody against prM. *Applied Microbiology and Biotechnology*, **99**, 5917–5927.

Mansfield K L, Horton D L, Johnson N, Li L, Barrett A D T, Smith D J, Galbraith S E, Solomon T, Fooks A R. 2011. Flavivirus-induced antibody cross-reactivity. *Journal of General Virology*, **92**, 2821–2829.

Nooraei S, Bahrulolum H, Hoseini Z S, Katalani C, Hajizade A, Easton A J, Ahmadian G. 2021. Virus-like particles: Preparation, immunogenicity and their roles as nanovaccines and drug nanocarriers. *Journal of Nanobiotechnology*, **19**, 59.

Orlinger K K, Hofmeister Y, Fritz R, Holzer G W, Falkner F G, Unger B, Loew-Baselli A, Poellabauer E M, Ehrlich H J, Barrett P N, Kreil T R. 2011. A tick-borne encephalitis virus vaccine based on the European prototype strain induces broadly reactive cross-neutralizing antibodies in humans. *Journal of Infectious Diseases*, **203**, 1556–1564.

Palomino-Tapia V A, Zavala G, Cheng S, García M. 2019. Long-term protection against a virulent field isolate of infectious laryngotracheitis virus induced by inactivated, recombinant, and modified live virus vaccines in commercial layers. *Avian Pathology*, **48**, 209–220.

Pierson T C, Fremont D H, Kuhn R J, Diamond M S. 2008. Structural insights into the mechanisms of antibody-mediated neutralization of flavivirus infection: Implications for vaccine development. *Cell Host & Microbe*, **4**, 229–238.

Prymula R, Pöllabauer E M, Pavlova B G, Löw-Baselli A, Fritsch S, Angermayr R, Geisberger A, Barrett P N, Ehrlich H J. 2012. Antibody persistence after two vaccinations with either FSME-IMMUN® Junior or ENCEPUR® Children followed by third vaccination with FSME-IMMUN® Junior. *Human Vaccines & Immunotherapeutics*, **8**, 736–742.

Rawat K, Kumari P, Saha L. 2021. COVID-19 vaccine: A recent update in pipeline vaccines, their design and development strategies. *European Journal of Pharmacology*, **892**, 173751.

Ruzek D, Avsic Zupanc T, Borde J, Chrdle A, Eyer L, Karganova G, Kholodilov I, Knap N, Kozlovskaya L, Matveev A, Miller A D, Osolodkin D I, Overby A K, Tikunova N, Tkachev S, Zajkowska J. 2019. Tick-borne encephalitis in Europe and Russia: Review of pathogenesis, clinical features, therapy, and vaccines. *Antiviral Research*, **164**, 23–51.

Salvo M A, Kingstad-Bakke B, Salas-Quinchucua C, Camacho E, Osorio J E. 2018. Zika virus like particles elicit protective antibodies in mice. *PLoS Neglected Tropical Diseases*, **12**, e0006210.

Slunge D, Boman A, Studahl M. 2022. Burden of tick-borne encephalitis, Sweden. *Emerging Infectious Diseases*, **28**, 314–322.

Süss J. 2011. Tick-borne encephalitis 2010: Epidemiology, risk areas, and virus strains in Europe and Asia — An overview. *Ticks and Tick-Borne Diseases*, **2**, 2–15.

Taba P, Schmutzhard E, Forsberg P, Lutsar I, Ljostad U, Mygland A, Levchenko I, Strle F, Steiner I. 2017. EAN consensus review on prevention, diagnosis and management of tick-borne encephalitis. *European Journal of Neurology*, **24**, e1214–e1261.

Le Thanh T, Andreadakis Z, Kumar A, Gómez Román R, Tollefsen S, Saville M, Mayhew S. 2020. The COVID-19 vaccine development landscape. *Nature Reviews Drug Discovery*, **19**, 305–306.

Xing Y, Schmitt H J, Arguedas A, Yang J. 2017. Tick-borne encephalitis in China: A review of epidemiology and vaccines. *Vaccine*, **35**, 1227–1237.

Zhang H, Jin H, Yan F, Song Y, Dai J, Jiao C, Bai Y, Sun J, Liu D, Wang S, Zhang M, Lu J, Huang J, Huang P, Li Y, Xia X, Wang H. 2022. An inactivated recombinant rabies virus chimerically expressed RBD induces humoral and cellular immunity against SARS-CoV-2 and RABV. *Virologica Sinica*, **38**, 244–256.

Zhang M, Jin H, Li Y, Jiao C, Huang P, Bai Y, Gong Z, Zhang H, Liu S, Wang H. 2023. Genetically engineered bacterial-like particles induced specific cellular and humoral immunity as effective tick-borne encephalitis virus vaccine. *Aggregate*, **4**, 305.

Zhang N, Li C, Jiang S, Du L. 2020. Recent advances in the development of virus-like particle-based flavivirus vaccines. *Vaccines* (Basel), **8**, 481.

Zhang X, Cui Z. 2023. Nanoparticle-based vaccines against zoonotic viruses: A review. *Zoonoses*, **3**, 47.

Zimna M, Brzuska G, Salát J, Svoboda P, Baranska K, Szewczyk B, Růžek D, Krol E. 2023. Functional characterization and immunogenicity of a novel vaccine candidate against tick-borne encephalitis virus based on Leishmania-derived virus-like particles. *Antiviral Research*, **209**, 105511.

Zlatkovic J, Stiasny K, Heinz F X. 2011. Immunodominance and functional activities of antibody responses to inactivated West Nile virus and recombinant subunit vaccines in mice. *Journal of Virology*, **85**, 1994–2003.

Executive Editor-in-Chief Dongming Zhao
Managing Editor Han Zhang